Electronic Supporting Information

Titania hollow nanospheres of size 28±1 nm using soft-template and their application for lithium-ion rechargeable batteries

Experimental Section

Polymeric micelles solution was prepared by dissolving the required amount of the polymer above in distilled water and then transferred to a volumetric flask to obtain a stock solution with a concentration of 0.5 gL^{-1}. The micelle solution was adjusted to pH 9 by using dilute NaOH. The micelle solution (10 mL) containing NH_3 (20 μL) was stirred for a few minutes followed by addition of desired amounts of TBOT (TBOT/PAA = 3 to 8) under vigorous stirring. The milky suspension was stirred at room temperature for an hour and aged at 90 °C for 48 h under static conditions. The composite particles were repeatedly washed with distilled water and ethanol and dried at 60 °C. In order to remove the polymeric template as well as to crystallize the shell wall, the composite particles were heated to 500 °C for 3 h in a muffle furnace under air.

The electrochemical performance of hollow titania nanospheres is evaluated by a standard method based on a TiO_2/Li half cell, where TiO_2 and lithium foil serve as positive and negative electrodes, respectively. For lithium insertion studies, the hollow titania nanosphere (5.0 mg) was mixed mechanically with teflonized acetylene black (TAB-2, 5.0 mg) and then the mixture was pressed on a stainless steel mesh as the current collector under a pressure of 500 kg/cm^2 and dried at 160 °C for 4 h under vacuum. The electrochemical characterizations were carried out by using CR-2032 coin type cells with lithium as anode. The electrolyte used was 1 M $LiPF_6$-EC:DMC (1:2 by volume, Ube Chemicals). The coin cell assembling was performed in a glove box filled with argon (dew point, lower than −80 °C). The galvanostatic charge–discharge tests of the coin cell were performed at the constant current density of 0.5 mAcm^{-2}. For investigating the reductive/oxidative potential of the tatania, cyclic voltammetry (CV) was carried out in glass cells with 3 electrodes. The titania electrode served as the working electrode and lithium metal foil was used for counter and reference electrodes with in 1.0 M $LiPF_6$-EC/DMC (3:7 vol.).

Characterization: Powder X-ray diffraction (SXRD) patterns were collected on a Rigaku Rint-ultima diffractometer with CuKα radiation (40 kV, 20 mA) from 0.7° to 5° 2θ in 0.01 steps at a scan speed of 1° min^{-1} and a Shimadzu XRD-7000 (WXRD) diffractometer. N_2 adsorption/desorption analyses were carried out by using a Belsorp-mini II (Bel Japan) apparatus. DLS measurements were carried out with an Otsuka ELS-8000 electrophoretic light scattering spectrophotometer. The TEM pictures were recorded on JEOL JEM-1210 (80 kV) and JEM-2100 (200 kV) electron microscopes. Fourier-transform infrared (FTIR) spectra were recorded on a Jasco FT/IR 7300 spectrometer by using a KBr pellet technique. Thermogravimetry and differential thermal analysis (TG-DTA) were obtained with a MAC Science TG-DTA 2100 instrument under air. Raman spectra were obtained by using a Jasco micro-Raman system NRS-3300 equipped with a holographic notch filter, 600 grooves/mm holographic grating, a 100X-microscope objective and peltier cooled (– 50 °C) CCD detector. UV-visible diffuse reflectance spectra were obtained on a Jasco V-650 spectrometer. Galvanostatic charge-discharge measurements were performed on a BTS 2004 equipment, Nagano charge/discharge instrument. CV measurements were performed using an HSV-100 appratus (Hokuto Denko Ltd., Japan).

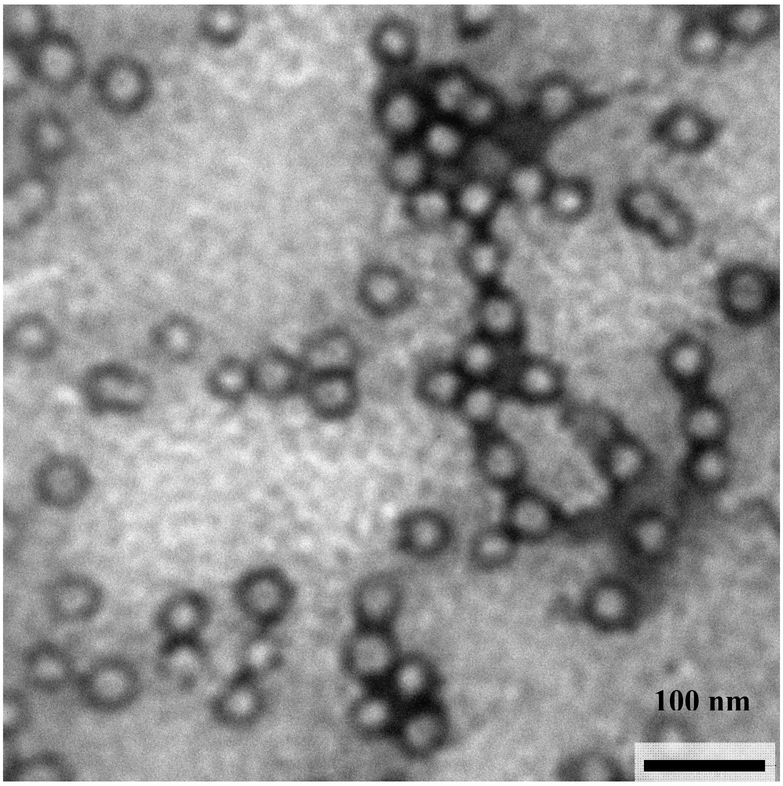

Fig. S1. TEM image of the micelles of PS–PAA–PEO stained with phosphotungstic acid.

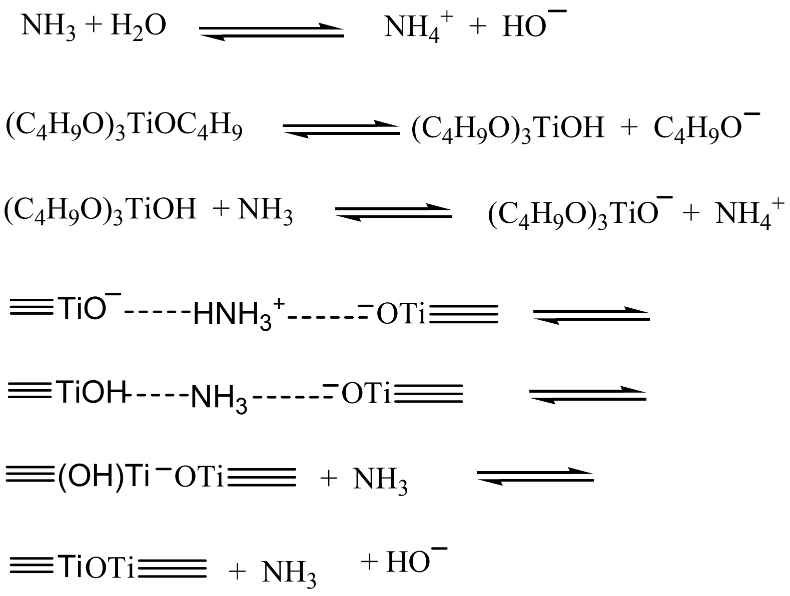

Scheme S1. Condensation of hydrolyzed titania species in the hollow shell structure in presence of ammonia catalyst.

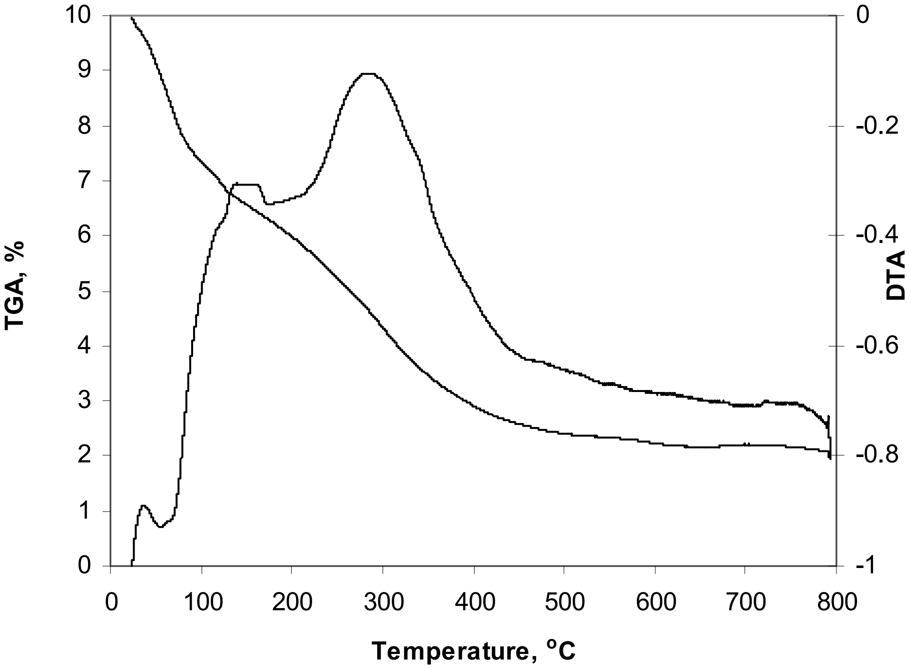

Fig. S2. TG/DTA curves of PS–PAA–PEO/titania composite particles

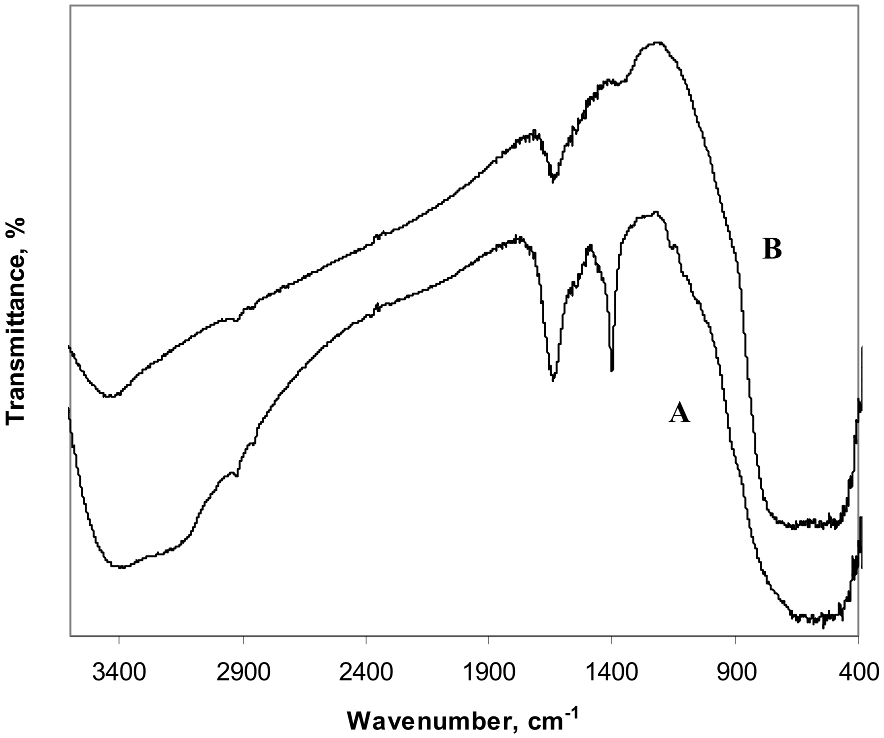

Fig. S3. FT IR spectra of: (A) Titania composite particles and (B) Calcined hollow titania nanospheres.

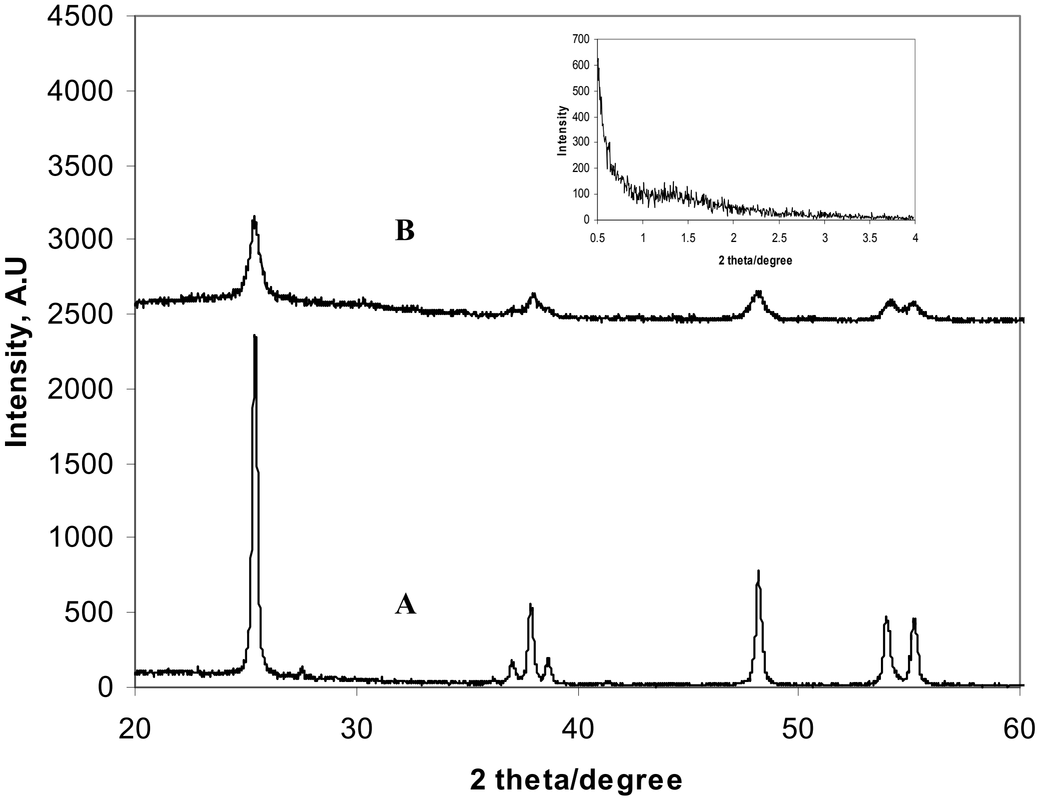

Fig. S4. Wide-angle XRD patterns of: (A) bulk titania and (B) hollow titania nanospheres. The inset figure corresponds to small-angle XRD of hollow titania nanspheres.

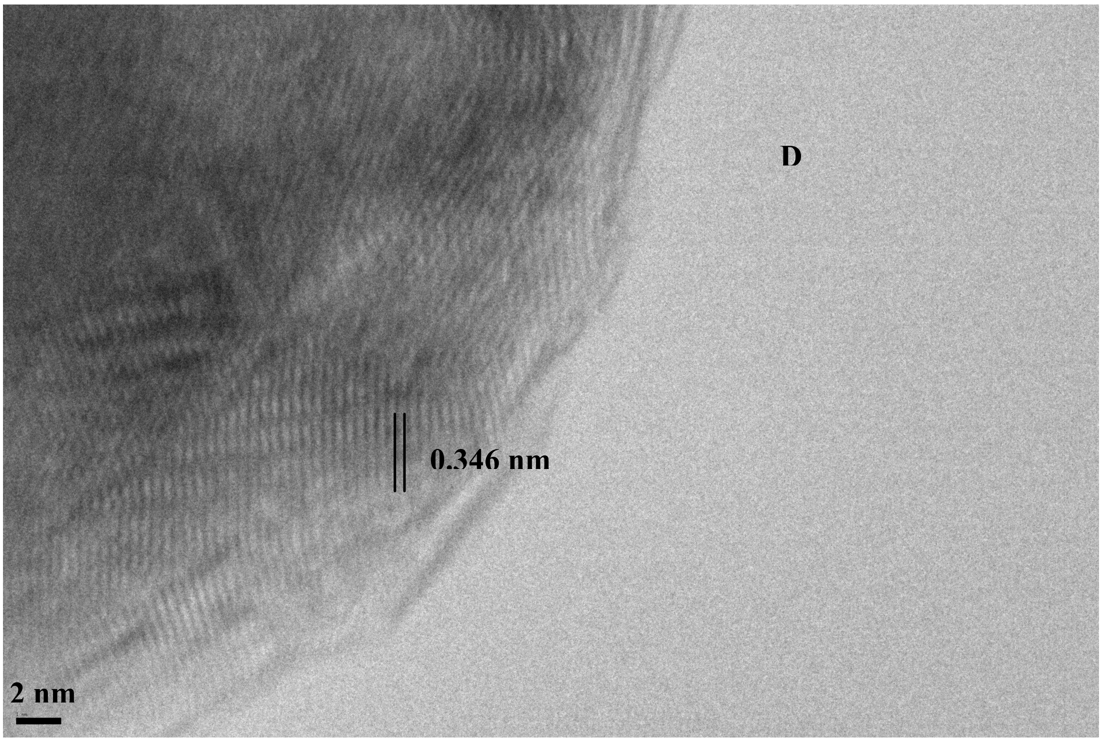

Fig. S5. High-resolution TEM of sample B.

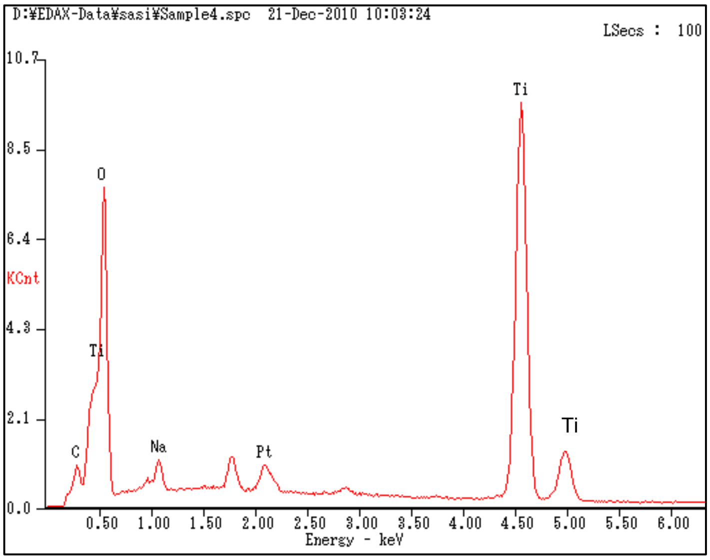

Fig. S6. EDX analysis of hollow titania nanospheres.

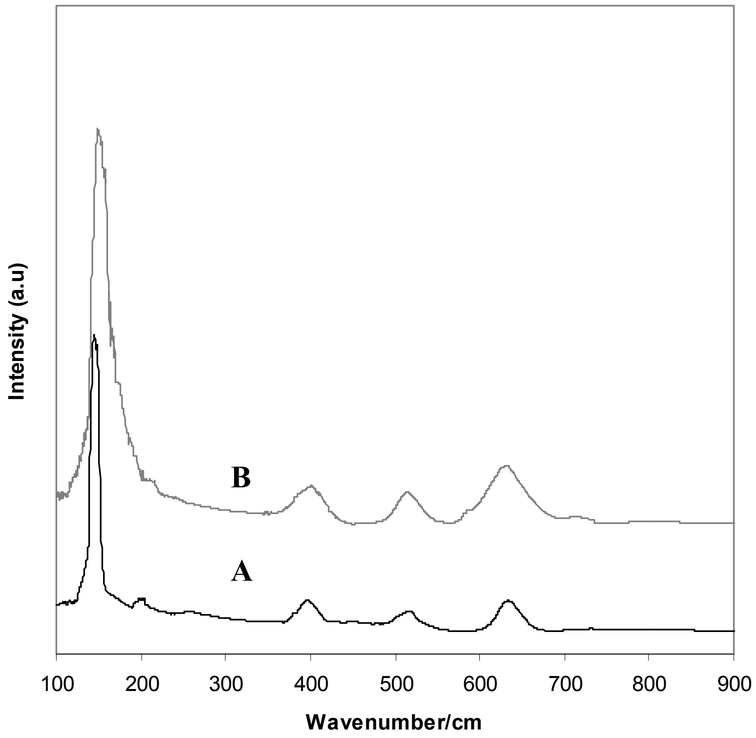

Fig. S7. Laser Raman spectra of: (A) bulk titania obtained by homogeneous precipitation and (B) hollow titania nanospheres.

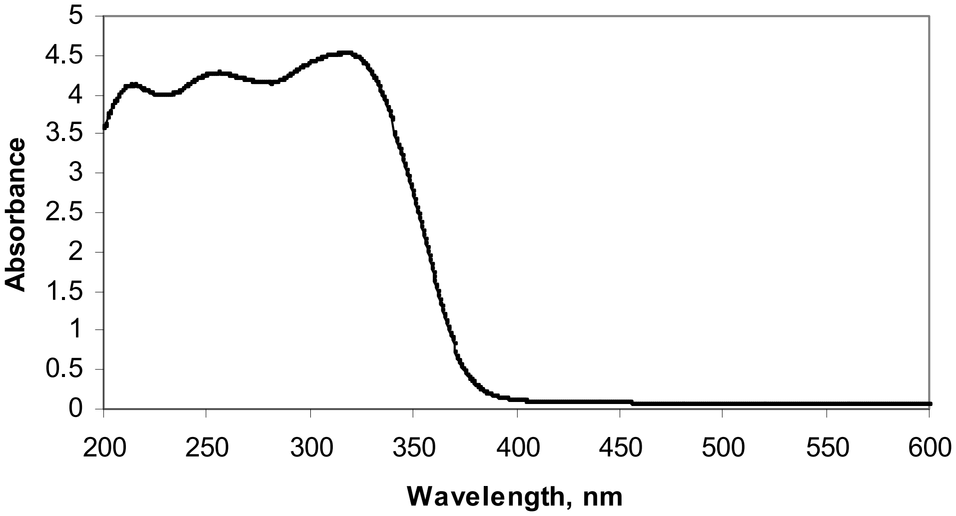

Fig. S8. UV-vis diffused reflectance spectra of hollow titania nanospheres.

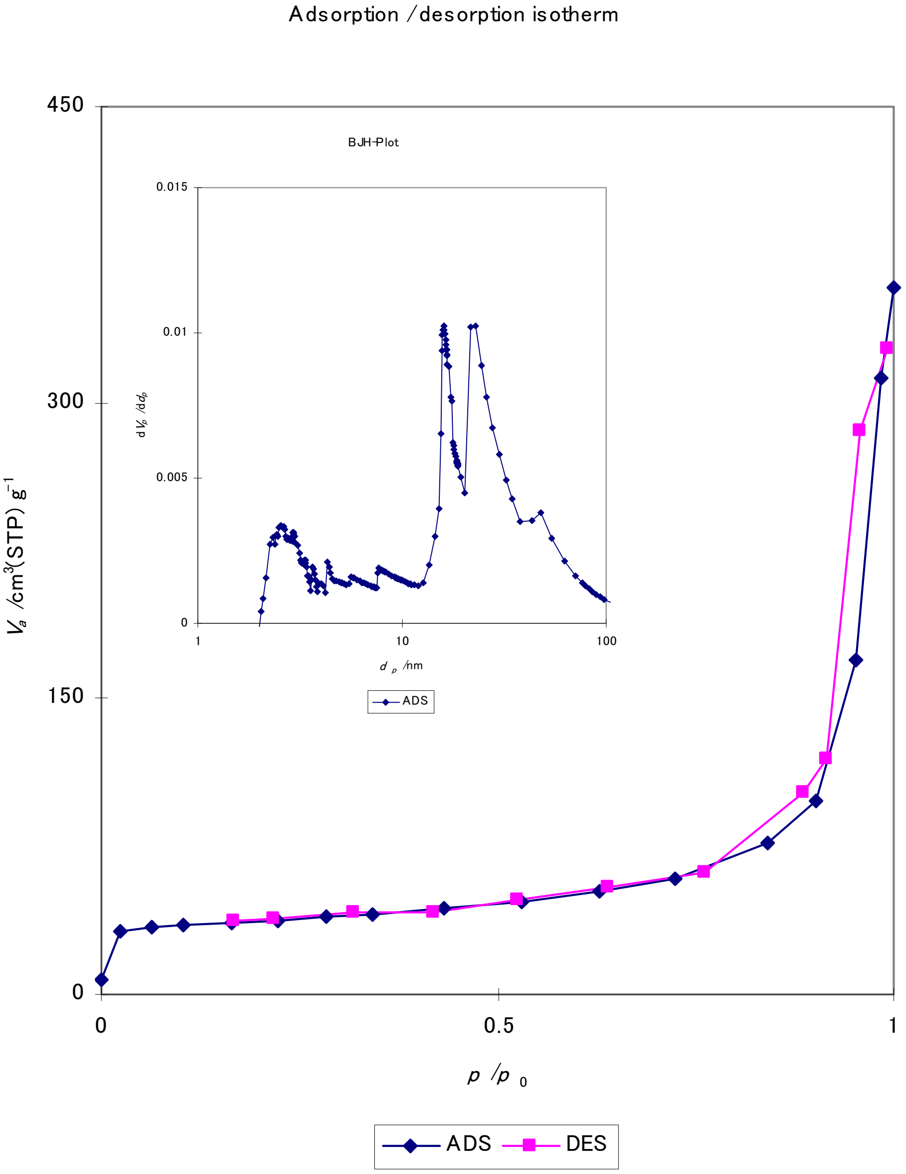

Fig. S9. Nitrogen adsorption/desorption isotherms of hollow titania obtained with PS–PAA–PEO and the inset figure shows pore-size analysis curve obtained by BJH mode.

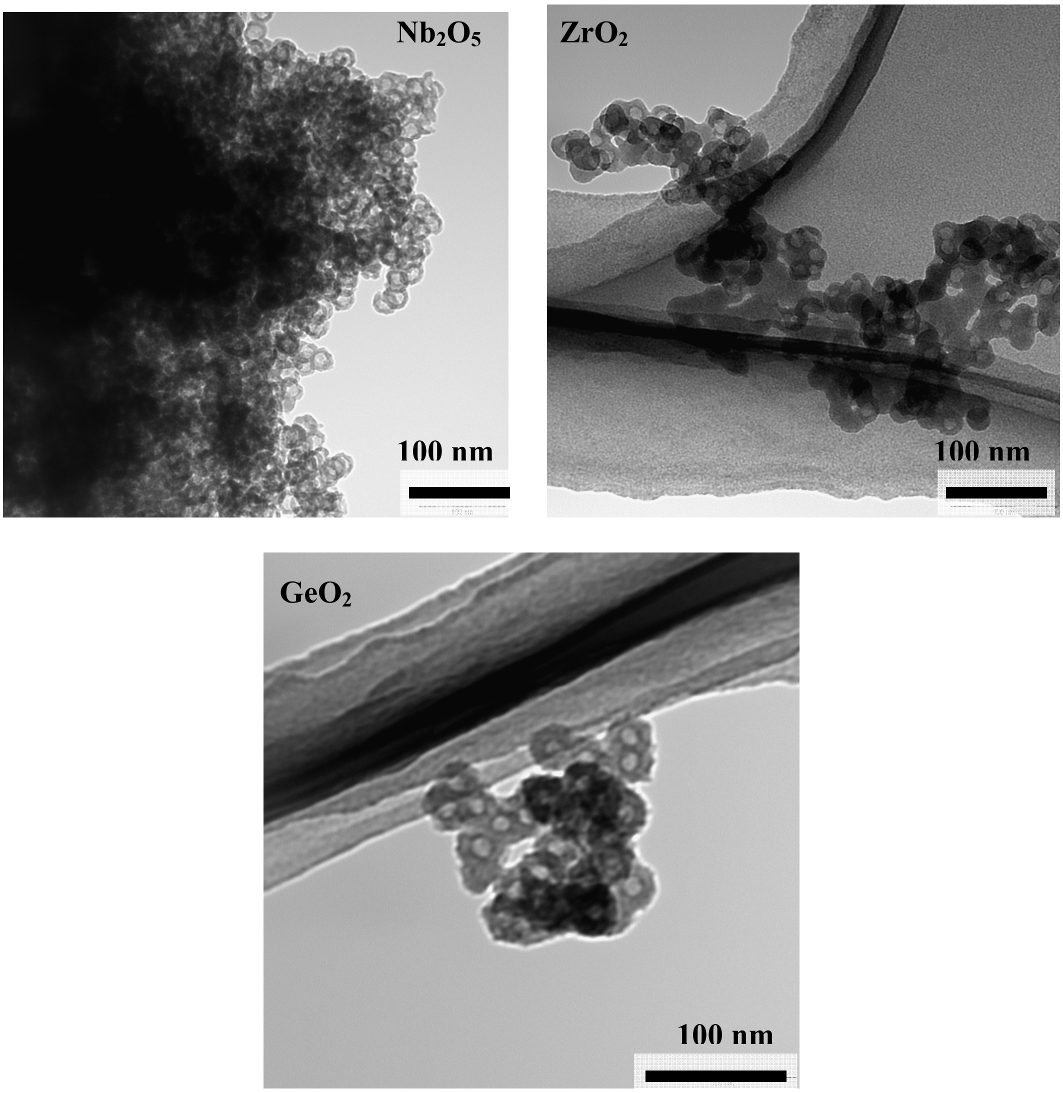

Fig. S10. TEM images of hollow metal oxide nanospheres with different compositions.

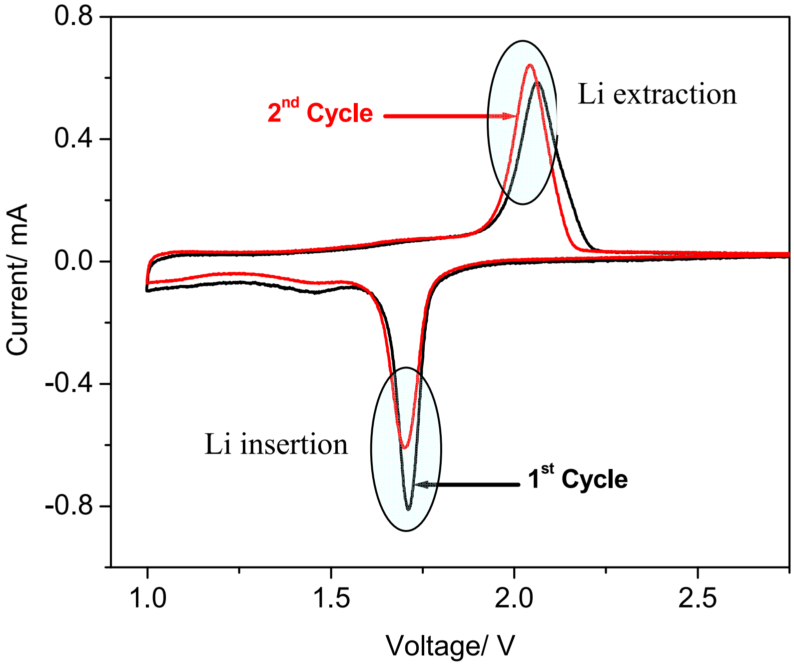

Fig. S11. cyclic voltammograms at a 5mV/min sweep rate.

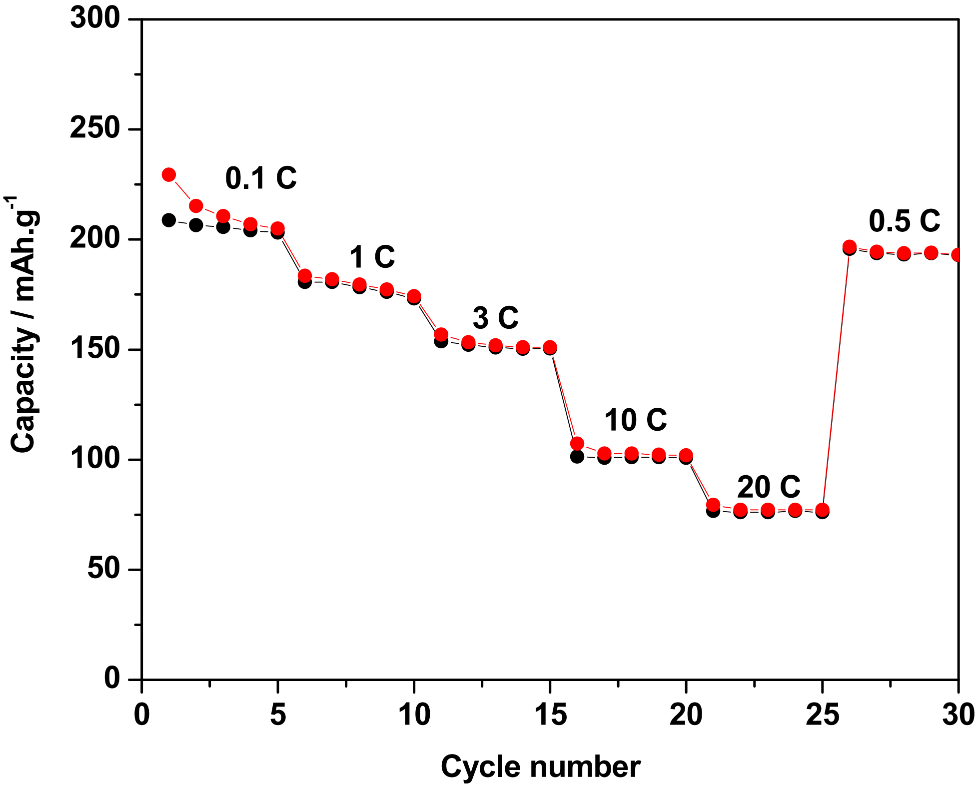

Fig. S12. Rate performance of hollow titania nanospheres